J. Mol. Model. **2000**, *6*, 618 – 629

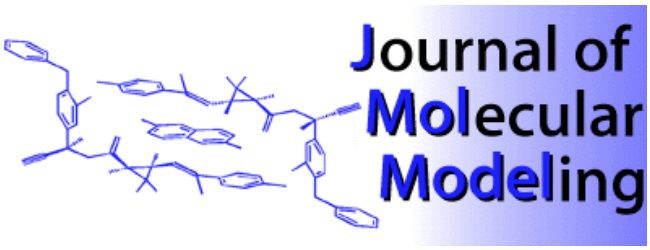

FULL PAPER

A CoMFA Study of Enantiomeric Organophosphorus Inhibitors of Acetylcholinesterase

Philippe P. Bernard[1], Dmitri B. Kireev[1], Marco Pintore[1], Jacques R. Chrétien[1], Pierre-Louis Fortier[2], and Daniel Froment[2]

[1]Laboratory of Chemometrics and BioInformatics, University of Orléans, BP 6759, F-45067 Orléans, France. Fax: +33-2-38 41 70 76. E-mail: jacques.chretien@univ-orleans.fr

[2]Centre d'Etudes du Bouchet, D.G.A., B.P. N°3, F-91710 Vert le Petit, France

Received: 2 February 2000/ Accepted: 29 June 2000/ Published: 13 December 2000

Abstract In a previous paper, presented by P. Bernard et al. [1], an automated docking was performed for stereospecific and quasi-irreversible organophosphorus acetylcholinesterase (AChE) inhibitors. In this study twelve chiral inhibitors, corresponding to six enantiomeric pairs, each with a phosphorus atom as a stereocenter, were docked to the crystal structure of mouse AChE. Then, the automated docking procedure was extended to a series of 35 organophosphorus compounds. The selected bioactive conformations derived from the docking procedure were used to establish a three dimensional model by means of the Comparative Molecular Field Analysis (CoMFA) method. In contrast to the conventional CoMFA studies, the compounds were not fitted to a reference compound but taken in their protein-based alignments derived from the docking study. For validation purposes, the established CoMFA model was then applied to another series of 24 organophosphorus compounds whose AChE inhibitory activity data were measured in different experimental conditions. A good correlation between predicted and experimental activity data shows that the model is robust and can also be extended to AChE inhibitory activity data measured on another acetylcholinesterase and/or at different incubation times and pH level.

Keywords Irreversible AChE inhibitors, CoMFA, Organophosphorus compounds

Introduction

The function of AChE is to recycle acetylcholine (ACh) by its hydrolysis at cholinergic synapses in order to restore the membrane potential after propagation of a nerve impulse [2]. AChE is a target enzyme for biologically active compounds ranging from anti-Alzheimer disease agents [3], acting as reversible inhibitors [4], to pesticides [5] and warfare agents, acting as reversible or irreversible inhibitors [6].

Many structure-activity data are currently available about the quasi-irreversible organophosphorus inhibitors that phosphorylate AChE at its catalytic site [7-10]. However, no general and reliable approach allowing to predict the AChE inhibitory activity of new organophosphorus inhibitors has yet been established. The known quantitative structure-activity relationships (QSAR) are limited to homogeneous series with

Correspondence to: J. R. Chrétien

structural variation at a single substitution site [11, 12]. AChE inhibitors bind themselves inside the enzyme and not on its surface. Hence, each point of an inhibitor's surface interacts with the enzyme, and even small structural changes, distant from the reacting functional group, may cause very important changes in the biological activity. This makes it impossible to derive a predictive model for the AChE inhibitory activity without a detailed understanding of how an inhibitor binds itself to the enzyme and what the structure of the enzyme's receiving cavity is.

A first attempt at giving a detailed description of the binding of the organophosphorus inhibitors to AChE was made by Järv [13]. It was based on the analysis of structure-activity data. His approach relied on already existing models of the substrate-enzyme interactions including interactions at the 'catalytic' site [14] and at the 'peripheral' site [15]. In its turn, the 'catalytic' site was subdivided into the 'esterasic' site, comprising among others the reacting serine residue, and the 'anionic' site, whose tryptophan residue interacts with the quaternary nitrogen of the choline fragment of ACh. Järv presented the catalytic site as a combination of distinct pockets, each of which receives an inhibitor's particular substituent (e.g. charged leaving group, non-charged leaving group, alkyl moiety). This discrete model explained many features of the organophosphorus ligand action. For example, after analyzing the ground state and the transition state geometries of the tetrahedral carbon and pentavalent phosphorus, Järv stated that the pocket receiving the leaving group of Ach is different from the one that accommodates the inhibitor leaving group.

More recent studies added new pockets to the 'pocket' model, which made it even fuzzier. Hosea et al. [16] recently suggested that in the mouse AChE the cationic organophosphonate leaving group binds itself to Asp 74, thus reinforcing Järv's hypothesis and 'creating' a new pocket, an anionic one. Then, Ordentlich et al. [17] showed that the *p*-nitrophenyl leaving group of paraoxon in the human AChE interacts with another pocket, an 'alkoxy' one formed by residues Trp86, Tyr337 and Phe338.

The increasing complexity of the 'pocket' model prompted us to investigate a new approach to the problem. The present availability of the three dimensional structure of AChE [18, 19], with the site-specific mutagenesis data [16, 17, 20-22] and the structure activity data [8] allowed us to construct a new three dimensional model for the cavity receiving the organophosphorus inhibitors. In this study, we applied the previously developed automated docking technique [23] to a series of six organophosphorus inhibitors, each with a stereocenter at the phosphorus atom in both *R* and *S* absolute configurations, in order to probe the space available for these compounds inside the enzyme. Firstly, this study aims to delineate a spatial model of the AChE catalytic cavity. The second issue concerns the structures of the inhibitor-enzyme complexes, these may be used as an input to the following 3D QSAR analyses.

This paper describes a special case in which, due to a 'critical' mass of available experimental data, it became possible to dock 35 organophosphorus AChE inhibitors to the catalytic site of the AChE with reasonable computational expenses. The docked inhibitors were then used in a protein-based alignment model to put on the CoMFA procedure [24,25]. This paper aims to show that docking of all compounds allows us to obtain a high quality, i.e. a robust 3D QSAR CoMFA model.

Methods

Biological data

Ligands For this work, we used 59 organophosphorus compounds. Their biological activities were measured by different research groups [9, 26-28]. These data included two subsets. The first one was formed by 35 organophosphorus compounds measured, in the same experimental conditions, on bovine erythrocyte acetylcholinesterase [26-28]. As the enzymatic measurements for these 35 organophosphorus compounds were taken at pH = 7.7 and 25 °C, the charged compounds were considered in their protonated forms. The second one included 24 organophosphorus compounds also measured in the same experimental conditions but on *Torpedo californica* acetylcholinesterase [9]. In both cases, the inhibitory activity of the compounds was expressed as K_i values.

Enzymes The crystal AChE structures were obtained from the Brookhaven Protein Data Bank (PDB). Currently, PDB has two types of 3D AChE structures available: (i) AChE from the *Torpedo californica* (PDB code: 1ACE) further referred to as TAChE and (ii) AChE from mouse (PDB code: 1MAH) further referred to as MAChE. The inhibitory activity data used in the present study are taken from measurements using bovine erythrocyte AchE, whose three dimensional structure is currently not available.

We studied the homology between a bovine AChE and those available in order to find out which available structure better fits the bovine enzyme. To carry out this comparison, we aligned together the primary sequences of MAChE, TAChE and the bovine AChE. At this stage it was found that MAChE and bovine AChE are easily superimposable. Superimposing the catalytic Ser203 of these two proteins aligns together almost the entire protein sequences (583 residues). A one by one comparison of these 583 residues revealed 44 differing residues.

The difference between TAChE and bovine AChE is much more significant. TAChE can be divided into three regions, each of which can be aligned with the corresponding region in bovine AChE. The links between these regions are different in the two enzymes. In total, within the three superimposable regions, which count 536 residues, the one by one comparison of residues revealed 232 differing residues. Two of the differing residues, Phe330→Tyr337 and Ile439→Pro446, are located close to the catalytic site and may interact with the inhibitors. It was recently shown that even rather insignificant mutations such as F295Y or E202Q

could cause a significant change in the enzyme activity [16, 22]. Thus, taking MAChE the object of our docking study decreased the risk of having non-pertinent results, since this enzyme is similar to the bovine one at the catalytic site.

A more detailed discussion concerning the differences between the structures of TAChE, MAChE and bovine AChE can be found in our previous paper [23].

Computational details

Ligands and enzyme Each of the 59 ligands was modeled using Sybyl software [29] on a Silicon Graphics *INDY R5000* station. The starting conformations were optimized by molecular mechanics algorithm using the Tripos Force Field[30]. The lowest energy conformations were found by means of the SYBYL/SEARCH option and then used as initial conformations for docking.

For the enzyme structure, the inhibitor was removed from the crystallographic MAChE/inhibitor complex and hydrogen atoms were added to the original PDB enzyme structure using the BIOPOLYMER module of Sybyl. Then, the geometry of the protein was optimized using the AMBER force field [31].

Automated docking - protein-based alignment The automated dockings were established for all the 59 organophosphorus compounds on MAChE. The procedure was carried out in the same way as in a previous paper [1], where a thorough analysis concerning finding the best conformation of an enzyme-ligand complex was reported. Briefly, a three step docking strategy was applied in order to optimize the use of available structural constraints, thus minimizing computational time.

(i) The first step was to dock AChE with its quaternary nitrogen anchored in the position of the edrophonium's quaternary nitrogen, because the position of this nitrogen was known thanks to the crystallographic data. The automated docking procedure consisted of reorienting the inhibitor inside the fixed enzyme while simultaneously twisting all rotatable bonds. The inhibitor was reoriented relatively to three coordinate axes with an angle step of 30°. Sybyl's SYSTEMATIC SEARCH was performed for each orientation of the inhibitor. The angle step for the search was 30° and the energy of the entire inhibitor-enzyme complex was calculated at each step. The position of the AChE carbonyl group resulting from this docking analysis then served as the center of the region probed for placing the inhibitors' phosphoryl group.

(ii) The second step was to find an appropriate position for the phosphoryl group. At this stage not only did we reorientate the inhibitor and twist the rotable bonds but we also translated it within the enzyme cavity. The systematic translation consisted of moving the phosphorous atom from one lattice intersection to another. The period of the lattice was 0.5 Å and it was limited by a cube with a 2 Å edge. This resulted in 125 lattice intersections within the cube. The center of the cube was placed onto the point identified at the first stage of the study as the position for the AChE carbonyl carbon atom. A bulky and very active organophosphorus inhibitor, the O-cyclopentyl, thiocholyl, methyl-phosphonate compound, was selected for the second stage.

(iii) At the third stage, the other inhibitors were docked to the enzyme. The position selected for the phosphorus atom at the second stage was used as the anchor point. The docking procedure was applied to these inhibitors in the same manner as it was applied to AChE at the first stage but using the phosphorus atom instead of the quaternary nitrogen as the anchor point.

The lowest energy complexes obtained in the course of the automated docking procedure were optimized using the AMBER force field.

CoMFA

Data set There were used 59 organophosphorus compounds, but two different experimental procedures were performed on them. So, a series was used as a training set and the other one as a test set. This avoided the random separation of the data set into a training set and test set. Moreover, the larger subset, in term of molecular diversity, was to be used as a training set in order to derive the better general model.

The training set and the corresponding biological data used in this study were selected from the literature [26-28]. The molecular structures and AChE inhibitory activity data of 35 organophosphorus compounds on bovine erythrocytes AChE are summarized in Table 1. All the collected biological data were measured under the same experimental conditions.

The test set was made of a new series of 24 organophosphorus compounds on *Torpedo californica* AChE [9] whose structure and activity data are presented in Table 2. This test set was used in the validation of the CoMFA model. The QSAR/ANALYSIS/PREDICT option of SYBYL was used to calculate the AChE inhibitory activity for these compounds.

CoMFA method A CoMFA study normally begins with searching for a suitable alignment of the molecules under investigation by using a constrained reference compound. In the present study this problem was *a priori* resolved by docking the compounds to the crystal AChE structure.

Both steric and electrostatic CoMFA fields were calculated using a sp^3 carbon atom as a probe, with a charge of +1 in the grid points around the molecules. The grid points were spaced by 1.0 Å in all three dimensions. Partial atomic charges for the electrostatic field calculation were obtained by the MOPAC AM1 method [32].The CoMFA region was chosen to include all the molecules with margins of at least 4.0 Å. The field values were truncated at +30 kcal/mol for steric and ± 30 kcal/mol for electrostatic interactions.

The Partial Least Squares method (PLS) [33] was used to relate the CoMFA fields to the inhibitory activity values linearly. The model quality was evaluated by the "leave-one-out" cross-validation procedure [34] and expressed in terms of Q^2, the cross-validated correlation coefficient, R^2, the conventional correlation coefficient, s, the standard error, and F, the Fisher test.

Table 1 *Structure-Activity data of the training set. X is leaving group. Conf indicates the enantiomeric conformation, considering as stereo-center the P atom. The experimental values for the inhibition constant K_i are derived from the references [26-28]*

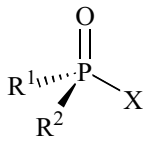

ID	X	R^1	R^2	Conf	K_i ($M^{-1}\cdot min^{-1}$)	log K_i
1	S-$CH_2CH_2CH(CH_3)_2$	O-iso-propyl	methyl	S	$7{,}0\cdot10^2$	2.85
2	S-CH_2CH_2F	O-iso-propyl	methyl	S	$7{,}0\cdot10^3$	3.85
3	S-$CH_2CH_2SCH_3$	O-iso-propyl	methyl	S	$2{,}0\cdot10^4$	4.30
4	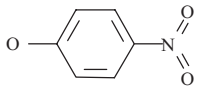	O-iso-propyl	methyl	S	$1{,}0\cdot10^6$	6.00
5	S-$CH_2CH_2N(CH_3)_2$	O-iso-propyl	methyl	S	$1{,}0\cdot10^7$	7.00
6	F	O-iso-propyl	methyl	S	$1{,}0\cdot10^7$	7.00
7	S-$CH_2CH_2S(CH_3)_2$	O-iso-propyl	methyl	S	$4{,}0\cdot10^7$	7.60
8	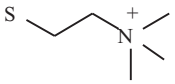	O-iso-propyl	methyl	S	$5{,}0\cdot10^7$	7.70
9	S-$CH_2CH_2N(CH_3)_2$	O-cyclopentyl	methyl	S	$7{,}0\cdot10^8$	8.85
10	F	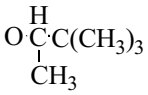	methyl	S	$2{,}0\cdot10^8$	8.30
11	F	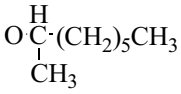	methyl	S	$4{,}0\cdot10^7$	7.60
12	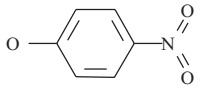	S-methyl	methyl	R	$2{,}0\cdot10^4$	4.30
13	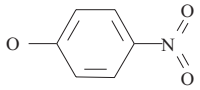	S-ethyl	methyl	R	$2{,}0\cdot10^5$	5.30
14	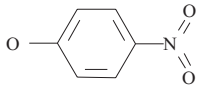	S-propyl	methyl	R	$2{,}0\cdot10^6$	6.30
15	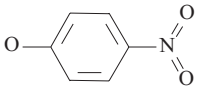	S-pentyl	methyl	R	$2{,}0\cdot10^6$	6.30
16	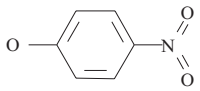	S-butyl	methyl	R	$3{,}0\cdot10^6$	6.48
17	S-$CH_2CH_2CH(CH_3)_2$	methyl	O-iso-propyl	R	$6{,}0\cdot10^2$	2.77
18	S-CH_2CH_2F	methyl	O-iso-propyl	R	$2{,}3\cdot10^3$	3.37
19	S-$CH_2CH_2SCH_3$	methyl	O-iso-propyl	R	$1{,}45\cdot10^4$	4.16

Table 1 (continued)

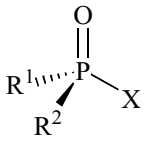

ID	X	R^1	R^2	Conf	K_i ($M^{-1}\cdot min^{-1}$)	log K_i
20	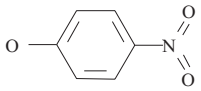	methyl	O-iso-propyl	R	$2,7\cdot10^3$	3.43
21	S-$CH_2CH_2N(CH_3)_2$	methyl	O-iso-propyl	R	$3,2\cdot10^3$	4.50
22	F	methyl	O-iso-propyl	R	$2,4\cdot10^4$	3.38
23	S-$CH_2CH_2S(CH_3)_2$	methyl	O-iso-propyl	R	$1,175\cdot10^5$	5.07
24	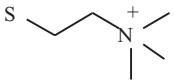	methyl	O-iso-propyl	R	$4,2\cdot10^4$	4.62
25	S-$CH_2CH_2N(CH_3)_2$	methyl	O-cyclopentyl	R	$2,1\cdot10^5$	5.32
26	F	methyl	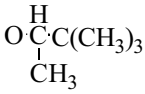	R	$1,15\cdot10^4$	4.06
27	F	methyl	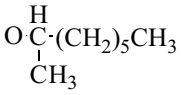	R	$1,0\cdot10^5$	5.01
28	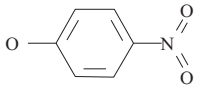	methyl	S-methyl	S	$1,6\cdot10^4$	4.22
29	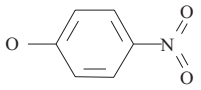	methyl	S-ethyl	S	$1,5\cdot10^4$	4.19
30	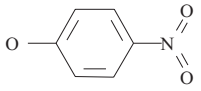	methyl	S-propyl	S	$5,5\cdot10^4$	4.75
31	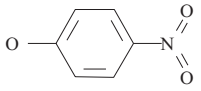	methyl	S-pentyl	S	$7,0\cdot10^4$	4.84
32	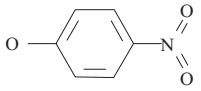	methyl	S-butyl	S	$6,0\cdot10^4$	4.77
33	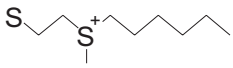	O-iso-propyl	methyl	S	$2,0\cdot10^6$	6.30
34	F	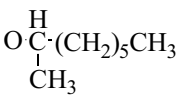	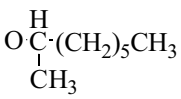	–	$2,0\cdot10^8$	8.30
35	S-$CH(CH_3)CH_2N(CH_3)_2$	O-ethyl	O-ethyl	–	$3,0\cdot10^5$	5.48

Table 2 *Description of the compounds of the test set with their experimental and predicted activity values. X is leaving group. Conf indicates the enantiomeric conformation, considering as stereo-center the P atom. The experimental values for the inhibition constant K_i are derived from the reference [9]*

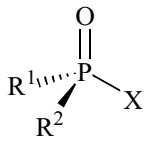

ID	X	R_1	R_2	Conf	K_i ($M^{-1}\cdot min^{-1}$) exp	log K_i exp	Log K_i pred
36	S-CH_3	O-cycloheptyl	methyl	S	$2{,}2\cdot10^5$	5.35	5.00
37	S-CH_3	methyl	O-cycloheptyl	R	$7{,}6\cdot10^2$	2.88	2.24
38	S-CH_2CH_3	O-cycloheptyl	methyl	S	$6{,}5\cdot10^3$	4.81	5.15
39	S-CH_2CH_3	methyl	O-cycloheptyl	R	$1{,}4\cdot10^1$	1.15	2.33
40	S-$(CH_2)_3CH_3$	O-cycloheptyl	methyl	S	$9{,}4\cdot10^4$	4.97	5.39
41	S-$(CH_2)_3CH_3$	methyl	O-cycloheptyl	R	$3{,}2\cdot10^1$	1.51	2.58
42	S-$(CH_2)_4CH_3$	O-cycloheptyl	methyl	S	$3{,}4\cdot10^5$	5.53	5.46
43	S-$(CH_2)_4CH_3$	methyl	O-cycloheptyl	R	$1{,}29\cdot10^2$	2.11	2.69
44	S-$(CH_2)_5CH_3$	O-cycloheptyl	methyl	S	$2{,}9\cdot10^4$	5.46	5.40
45	S-$(CH_2)_5CH_3$	methyl	O-cycloheptyl	R	$1{,}14\cdot10^2$	2.06	2.80
46	S-CH_3	O-iso-propyl	methyl	S	$3{,}17\cdot10^2$	2.50	2.87
47	S-CH_3	methyl	O-iso-propyl	R	$1{,}5\cdot10^1$	1.18	2.76
48	S-CH_2CH_3	O-iso-propyl	methyl	S	$7{,}5\cdot10^1$	1.85	2.77
49	S-CH_2CH_3	methyl	O-iso-propyl	R	$2{,}9\cdot10^1$	1.46	2.79
50	S-$(CH_2)_4CH_3$	O-iso-propyl	methyl	S	$1{,}5\cdot10^3$	3.18	3.27
51	S-$(CH_2)_4CH_3$	methyl	O-iso-propyl	R	$2{,}6\cdot10^3$	3.42	3.13
52	S-$(CH_2)_5CH_3$	O-iso-propyl	methyl	S	$3{,}6\cdot10^3$	3.56	3.20
53	S-$(CH_2)_5CH_3$	methyl	O-iso-propyl	R	$3{,}0\cdot10^1$	1.48	3.45
54	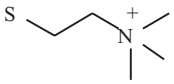	O-cycloheptyl	methyl	S	$3{,}0\cdot10^8$	8.48	8.76
55	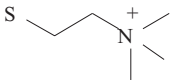	methyl	O-cycloheptyl	R	$1{,}4\cdot10^6$	6.20	6.18
56	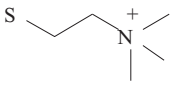	O-iso-propyl	methyl	S	$1{,}3\cdot10^7$	7.11	7.78
57	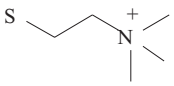	Methyl	O-iso-propyl	R	$8{,}7\cdot10^4$	4.94	4.68
58	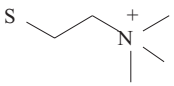	O-$(CH_2)_2C(CH_3)_3$	methyl	S	$1{,}0\cdot10^9$	9.00	8.93
59	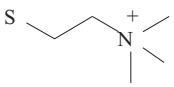	Methyl	O-$(CH_2)_2C(CH_3)_3$	R	$3{,}3\cdot10^7$	7.52	6.96

Results and discussion

Automated docking – protein-based alignment

The automated docking for a series of *S*- and *R*-enantiomers of 59 organophosphorus irreversible inhibitors of acetylcholinesterase indicates that the leaving group in the Michaelis complex is directed towards the entry of the active site (Asp74). This orientation supports an effective in-line attack of the phosphorus atom, as recently suggested by Hosea et al [16, 22]. Figure 1 shows the 59 organophosphorus compounds superimposed in their relative natural alignment. This alignment was selected to create the CoMFA model. This protein-based alignment allowed us to interpret the shift of the phosphoryl group from one *R/S*-configuration to another in each couple of compounds. This shift is probably responsible for the differences in activity between the enantiomeric forms. The shift is due to the bad arrangement of the substituents around the phosphorus atom. For example, in the case of the *R*-enantiomer of compound 24, the O-isopropyl group cannot occupy the acyl pocket [16, 17], this resulting in a shift of the P=O group. This is not the case for the corresponding *S*-enantiomer for which the acyl pocket accommodates the methyl group very well.

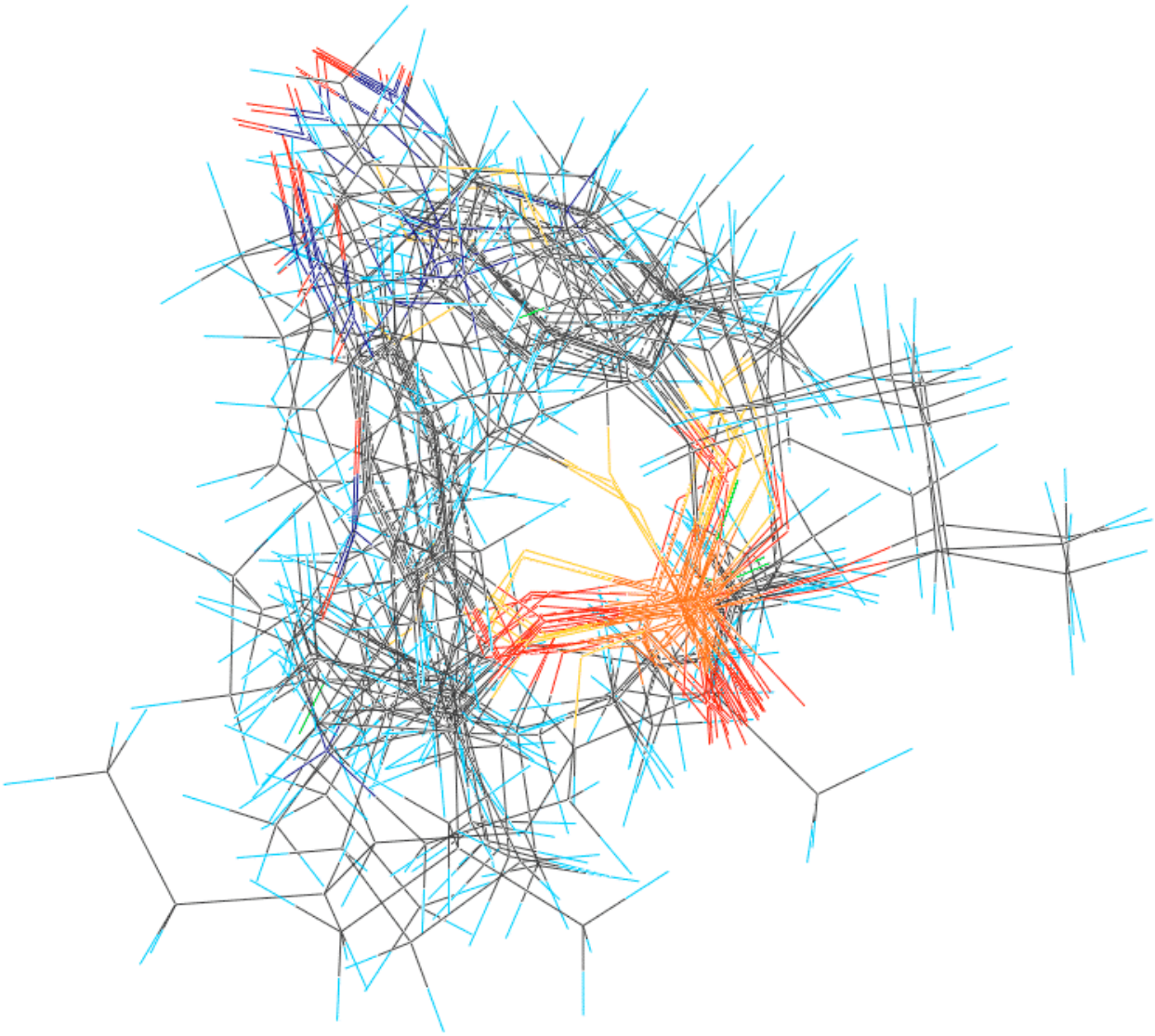

Figure 1 *Protein-based alignment of 59 enantiomeric irreversible organophosphorus compounds. The complex AChE - compound* ***9*** *was used as template to perform the alignment*

CoMFA model

The present CoMFA study is particular in that each of the 35 organophosphorus compounds studied was aligned in an independent way. No reference compound was used and the geometrical arrangements of the inhibitors were only selected by interactions with the biological receptor. The protein-based alignment without a reference compound may have an impact on the nature of the structural information we expect to obtain from the CoMFA analysis. A good statistic and predictive quality of the CoMFA model normally suggests that the molecules in the real biological system are aligned in accordance with the initial alignment of the CoMFA procedure. In the present case, as the alignment was prepared using the structure of the receptor as a template, the good quality of the CoMFA model would suggest the validity of the proposed model of inhibitor-enzyme interactions obtained by the automated docking procedure.

For a better understanding of the factors that underlie the activity, three different CoMFA models were built: (i) a model with only a steric field, (ii) a model with an electrostatic field and (iii) a model taking both fields into account. The results of these analyses are presented in Table 3, where N and n_{PC} represent the total number of compounds and the optimal number of PLS components, respectively. Table 3 underlines the importance of both the CoMFA steric and electrostatic fields. Indeed, the analysis including both fields shows that the relative contributions to the model are 47% for the steric field and 53% for the electrostatic one. Thus, in the present study, the model comprising both steric and electrostatic fields (Q^2 = 0.70) was finally taken to plot the CoMFA statistic

Table 3 *Statistics and cross-validation results of the three CoMFA models. N is the total number of compounds considered; n_{PC} represents the number of principal components; Q^2 and R^2 indicate the correlation coefficients with and without cross-validation, respectively; F is the Fisher test value; sd represents the standard deviation*

	Steric	Electrostatic	Steric and Electrostatic
N	35	35	35
n_{PC}	5	5	5
Q^2	0.61	0.47	0.70
R^2	0.96	0.96	0.98
F	205	170	312
sd	0.30	0.33	0.22

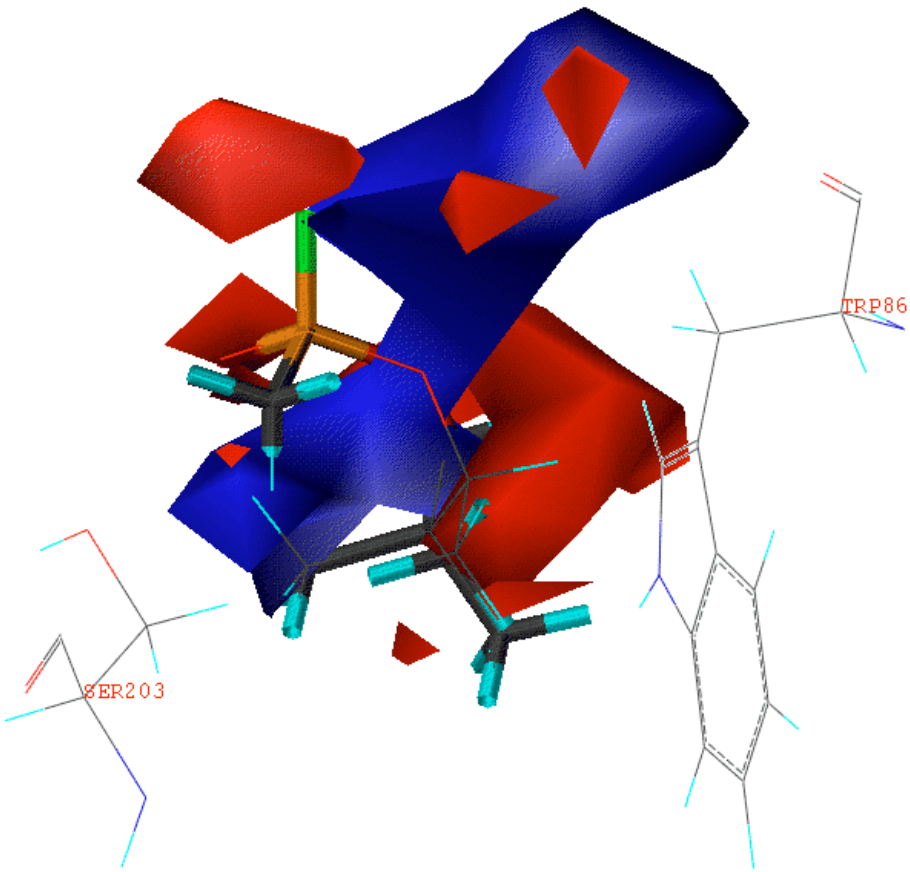

Figure 2 *CoMFA electrostatic field plot for compound **10**. Increasing the negative charge inside the red regions and the positive charge in the blue regions favor the inhibitory activity. Some residues belonging to the acetylcholinesterase catalytic site are shown*

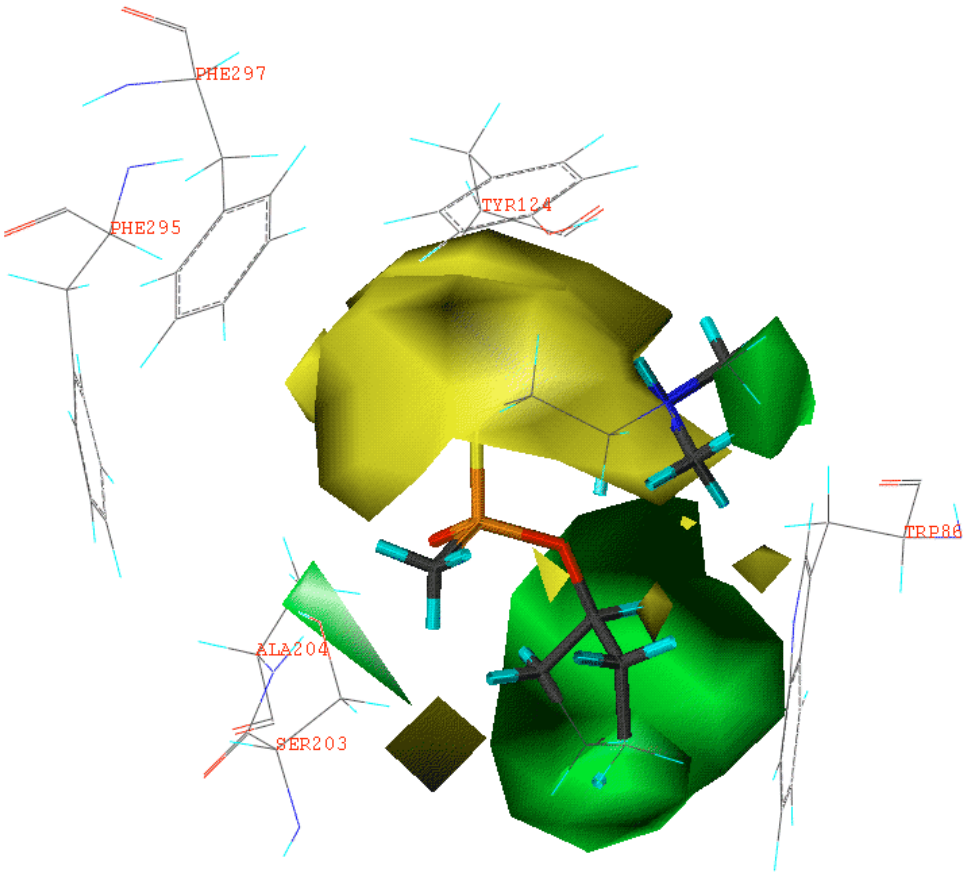

Figure 3 *CoMFA steric field plot for compound* ***9****. Increasing the bulk effect inside the green regions and decreasing the bulk effect inside the yellow regions favor the inhibitory activity. Some residues belonging to the acetylcholinesterase catalytic site are shown*

fields and to predict the AChE inhibitory activity for new compounds.

Finally, a non cross-validated PLS run was performed in order to generate the final CoMFA plots. These plots outline a CoMFA statistic field, which expresses the relationship between the variations of the steric and electrostatic fields and the variation of the biological activity. The values of the fields are calculated at each lattice intersection and are equal to the product of the descriptor coefficient by the corresponding standard deviation (P_{SC} = STDEV·COEFF). Hence, an extremely low value of P_{SC} indicates that the presence of the corresponding steric or electrostatic field is not desirable at this point because its causes a decrease in activity. New molecules should not contain fragments that generate such a field in the lattice intersections with low P_{SC}. A high value of P_{SC} means that the corresponding field is desirable in this point and that the fragments that produce such a field are contributing to the activity. A P_{SC} plot for the electrostatic field is shown in Figure 2 and a plot for the steric field is presented in Figure 3. The chosen contour levels for the plots were 80% for the favorable region and 20% for the unfavorable one.

Two active compounds, **9** and **10**, of the training set illustrate the main features of the CoMFA plots. Some of the colored regions on the plots mark essential ligand-protein interactions. For instance, for the electrostatic field given for compound **10**, in Figure 2, a red sphere that envelopes the leaving group of the inhibitor, here the fluorine atom, is in agreement with the fact that a greater negative charge of this type of atom favors the breaking of the P-atom bond and then the departure of the leaving group. Furthermore, the blue volume around the small non-leaving methyl group is replaced by a crowded OR group in the *R*-configuration occupied by the O-cyclopentyl group. This negatively charged group is less favorable. It contributes to explain here the lower activity of the *R*-enantiomer versus the S one. The green surface in Figure 3 corresponding to the steric field of compound **9** is surrounding the O-cyclopentyl group and the cationic nitrogen. It is in favor of attachment of bulky substituents in these regions. Compounds **27** and **33** from Table 1 are in agreement with this fact. In addition, substitutions near the methyl group and above the organophosphorus compound are sterically unfavorable. This yellow region is explained by the presence of such residues as Phe295 and Phe297 of the enzyme, which limits the cavity size in this area.

Predictive aspect of the CoMFA model

After validating our model by means of cross-validation, the next step of the investigation consisted in applying the model to another series of AChE inhibitors whose activity is well-

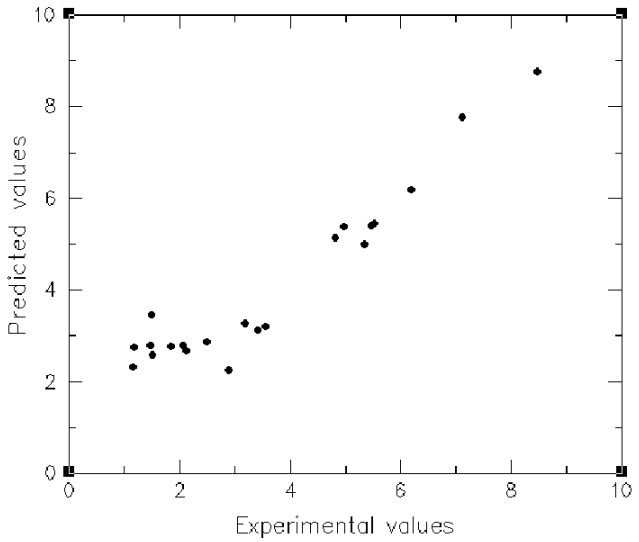

Figure 4 *LogK_i predicted values versus the experimental [9] ones for the 24 compounds of the test set (correlation coefficient R^2 = 0.90, standard deviation sd = 0.74, Fisher test F = 208)*

known. However, in view of the difficulty to find standard biological data on stereospecific organophosphorus compounds, the experimental values of the test set were measured in experimental conditions which differed from those in which the compounds of the training set were tested. The compounds of the training set were experimentally tested in the same conditions as the test set. The difference concerns the enzyme source. Bovine erythrocyte AChE was used for the training set, whereas *Torpedo californica* AChE was used for the test set. Due to the differences in this enzyme, the series of 24 compounds could have been considered as ineligible for the training set. Our previous paper [23] indicated that two different experimental conditions, in term of enzyme source and enzymatic assay, generate a shift in the predictivity of the QSAR model for the *N*-benzyl-piperidine derivatives which were another type of AChE inhibitors of interest.

The purpose of this step was to validate the model and simultaneously to explore the area of its applicability. Another important issue was the compatibility between the data measured in different experimental conditions. A variety of approaches to this problem may be found in literature. In a recent CoMFA study [35], the data measured on two different proteins (mouse and human AChE) were used both in the same training set and in separate ones. CoMFA models of comparable quality were obtained in both cases. In the latest source [36], special care was taken to provide compatibility. All the data were measured on the same enzyme, the *Torpedo californica* one, and two reference compounds were used to prove the compatibility of the data.

However, using one or two reference compounds cannot completely justify merging different series. For example, in the experimental study [37], the AChE inhibitory activity (IC_{50}) of tacrine is 81 nM. In another study [38] the activity of tacrine is 170 nM, which is relatively close to 81 nM. It may be concluded that the data from these two sources are compatible. Nevertheless, using physostigmine as a reference compound leads to a much less optimistic conclusion. Physostigmine has an AChE activity of 0.69 nM in one of the studies [37] and 19 nM in another study [39], which makes a 28-fold difference between the values. One may argue that some experimental parameters in the two aforementioned studies were different and that taking data measured in the same conditions would ensure compatibility, whatever the laboratory issuing the data may be. Experience shows, however, that the experimental conditions in different laboratories are rarely the same [3, 37, 40, 41]. More specifically, the combination of four, most important, experimental parameters such as the enzymatic assay methodology, the source of the enzyme, the pH level and the pre-incubation time differ from one laboratory to another.

The structural formulae, the predicted and real activity values with the corresponding deviations for the above 24 organophosphorus compounds are shown in Table 2. Figure 4 illustrates how tightly the predicted values correlate with the actual activity value (R^2 = 0.90). It means that the relative inhibitory capacities are correctly predicted for the whole series of 24 molecules. In addition, a parameter that is widely used to estimate the quality of test set predictions, *i.e.* PRESS/SSY [42], has also a good value of 0.1, which indicates a small deviation of the predicted values in comparison with the actual ones.

Three remarks may be derived from this part of the study. (i) First, the tight correlation between the predicted and the experimental values used in this study suggests that the present model is able to provide reliable predictions of the AChE inhibitory capacities in a set of new inhibitors. The good correlation between predicted and observed values also indicates a good predictive capacity of the present CoMFA model. (ii) The second remark deals with the non-shifted predictions for these 24 compounds. Indeed, from what was previously reported about reversible AChE inhibitors [23] and in view of the difference in the enzyme source used in this study, a shift between predictive and calculated activity values of the compounds might have been expected. These results suggest that even if the primary structure of an AChE is more or less variable according to its source, its catalytic behavior towards these organophosphorus compounds remains approximately the same. In addition, the shift obtained with the benzylpiperidines [23] may be due to different conditions in which the enzymatic assay was performed. Another explanation would consist in saying that benzylpiperidines, which are bulkier than organophosphorus compounds and occupy a large part of the catalytic site, are probably more sensitive to the structure variation of the enzyme. (iii) Finally, the predictive aspect of this model indicates that prediction is better for the most active compounds than for the least active ones. We can compare, in Table 2, compounds numbers **39**, **41**, **47**, **4**9 and **53**, the least active, and compounds numbers **38**, **44**, **58**, **58** and **56** which are the most active. The result could be explained by the fact that the least active compounds presented

more possible conformations during the docking study [1] than the most active ones. The latter presented no more than two conformational solutions whereas the inactive ones presented from six to ten solutions. Globally, the number of conformational solutions increases with the decrease in the activity of the compounds. This fact is related to the well known problem of entropy contribution and appraisal in computational chemistry.

Conclusion

An automated docking study was performed on a series of irreversible organophosphorus AChE inhibitors. Spatial constraints issued from the protein crystallographic data were initially imposed in order to reduce the research space. Due to these constraints, a reliable docking was performed for all the 59 molecules studied, with reasonable computational expenses.

The docking data were then used to proceed with the Comparative Molecular Field Analysis (CoMFA). According to the cross-validation test, this CoMFA model with a protein-based alignment has a high predictive capacity.

An independent series of 24 organophosphorus compounds, whose AChE activities were measured on another AChE, was used to study the area of the model applicability. The relative inhibitory capacities were correctly predicted for all the 24 molecules.

This robust and predictive 3D QSAR model of the AChE inhibitory activity might further be used for a better understanding of the molecular interactions between acetylcholinesterase and its irreversible inhibitors. Compared to the natural substrate, acetylcholine, the 3D model defines new areas within the catalytic site. Thus, this model could be used for designing antidotes against organophosphorus intoxication. This work is underway.

References

1. Bernard, P.; Kireev, D.B.; Chretien, J.R.; Fortier, P.-L.; Coppet, L. *J. Mol. Model.* **1998**, *4*, 323.
2. Nachmansohn, D. *Proc. Natl. Acad. Sci. U. S.* **1968**, 61, 1034.
3. Sugimoto, H.; Iimura, Y.; Yamanishi, Y.; Yamatsu, K. *Bioorg. & Med. Chem. Lett.* **1992**, 2, 871. Villalobos, A.; Blake, J.F.; Biggers, C.K.; Butler, T.W.; Chapin, D.S.; Chen, Y.L.; Ives, J.L.; Jones, S.B.; Liston, D.R.; Nagel, A.A.; Nason, D.M.; Nielsen, J.A.; Shalaby, I.A.; Frost White, W. *J. Med. Chem.* **1994**, 37, 2721.
4. Sugimoto, H.; Tsuchiya, T.; Sugumi, H.; Higurashi, K.; Karibe, N.; Iimura, Y.; Sasaki, A.; Kawakami, Y.; Araki, S.; Yamanishi, Y.; Yamatsu, K. *J. Med. Chem.* **1992**, 35, 4542.
5. Sanborn, J.R.; Fukuto, T.R. *J. Agr. Food Chem.* **1972**, 20, 926.
6. Froede, H.C.; Wilson, I.B. in *The enzymes*, Boyer, P.D., Ed., Vol. 5, 3rd ed., Academic Press, New York and London, 1971, pp 87-114.
7. Aldridge, W.N.; Reiner, E. *Enzyme inhibitors as substrates*, North Holland Publishing Co., Amsterdam, The Netherlands, 1972.
8. Ariëns, E.J.; van Rensen, J.J.S.; Welling, W. (Editors), *Stereoselectivity of pesticides; biological and chemical problems*, Elsevier Science Publishers B. V., Amsterdam, 1988.
9. Berman, H.A.; Leonard, K. *J. Biol. Chem.* **1989**, 29, 3942.
10. Brestkin, A.P.; Godovikov, N.N. *Russian Chem. Rew.* **1978**, 47, 859.
11. Gupta, S.P.; Singh, P. *Indian Journal of Chemistry* **1979**, 17B, 605.
12. Ashman, W.P.; Groth M.J. In *Proceedings of the scientific conference on chemical and biological defense*, 1995.
13. Järv, J. *Bioorganic Chemistry* **1984**, 12, 259.
14. Nachmansohn, D.; Wilson, I.B. *Adv. Enzymol.* **1951**, 12, 259.
15. Bergmann, F.; Wilson, I.B.; Nachmansohn, D. *Biochim. Biophys. Acta* **1950**, 6, 217.
16. Hosea, N.A.; Radic, Z.; Tsigelny, I.; Berman, H.A.; Quinn, D.M. Taylor, P. *Biochemistry* **1996**, 35, 10995.
17. Ordentlich, A.; Barak, D.; Kronman, C.; Ariel, N.; Segall, Y.; Velan, B.; Shafferman, A. *J. Biol. Chem.* **1996**, 271, 11953.
18. Sussman, J.L.; Harel, M.; Frolow, F.; Oefner, C.; Goldman, A.; Toker, L.; Silman, I. *Science* **1991**, 253, 872.
19. Bourne, Y.; Taylor, P.; Marchot, P. *Cell* **1995**, 83, 503.
20. Radic, Z.; Pickering, N.A.; Vellom, D.C.; Camp, S.; Taylor, P. *Biochemistry* **1993**, 32, 12074.
21. Ordentlich, A.; Barak, D.; Kronman, C.; Flashner, Y.; Leitner, M.; Segall, Y.; Ariel, N.; Cohen, S.; Velan, B.; Shafferman, A. *J. Biol. Chem.* **1993**, 268, 17083.
22. Hosea, N.A.; Berman, H.A.; Taylor, P. *Biochemistry* **1995**, 34, 11528.
23. Bernard, P.; Kireev, D.B.; Chretien, J.R.; Fortier, P.L.; Coppet, L. *J. Comput.-Aided Molecular Design* **1999**,13, 355.
24. Bromidge, S.M.; Dabbs, S.; Davies, D.T.; Duckworth, D.M.; Forbes, I.T.; Ham, P.; Jones, G.E.; King, F.D.; Saunders, D.V.; Starr, S.; Thewlis, K.M.; Wyman, P.A.; Blaney, F.E.; Naylor, C.B.; Bailey, F.; Blackburn, T.P.; Holland, V.; Kennett, G.A.; Riley, G.J.; Wood, M.D. *J. Med. Chem.* **1998**, 41, 1598.
25. Matter, H.; Schwab, W.; Barbier, D.; Billen, G.; Haase, B.; Neises, B.; Schudok, M.; Thorwart, W.; Schreuder, H.; Schreuder, H.; Brachvogel, V.; Lönze, P; Weithmann, K.U; *J. Med. Chem.* **1999**, **42**, 1908.
26. Keijer, J.H.; Wolring, G.Z. *Biochim. Biophys. Acta* **1969**, 185, 465.
27. Boter, H.L.; de Jong, L.P.A.; Kienhuis, H. In Edery, H., Klingberg, M.A. and Turner, I. (Eds) *Proceedings of the 'Oholo' 16th Annual Biology Conference. Interaction of chemical agents with cholinergic mechanisms*, Israel Institute for Biological Research, Ness-Ziona, Israel, 1971.

28. Ooms, A.J.J.; Boter, H.L. *Biochem. Pharmacol*. **1965**, 14, 1839.
29. Sybyl 6.5 is available from Tripos Associates, 1699 South Hanley Road, St Louis, MO 63144.
30. Clark, M.; Cramer, R.D.III; Opdenbosch, N.V. J. Comput. Chem. **1989**, 10, 982.
31. Weiner, S.J.; Kollman, P.A.; Nguyen, D.T.; Case D.A. *J. Comp. Chem.* **1986**, 7, 230.
32. Dewar, M.J.S.; Zoebich, E.G.; Healy, E.F.; Stewart, J.J.P. *J. Amer. Chem. Soc.* **1985**, 107, 3902.
33. Wold, S. In *Chemometric Methods in Drug Design*, van de Waterbeemd, H., Ed.; VCH, Weinheim, 1995, pp 195-218.
34. Wold, S.; Eriksson, L. In *Chemometric Methods in Drug Design*, van de Waterbeemd, H., Ed.; VCH, Weinheim, 1995, pp 309-318.
35. Tong, W.; Collantes, E.R.; Chen, Y.; Welsh, W. *J. Med. Chem.* **1996**, 39, 380.
36. Cho, S.J.; Serrano Garcia, M.L.; Bier, J.; Tropsha, A. *J. Med. Chem.* **1996**, 39, 5064.
37. Sugimoto, H.; Tsuchiya, T.; Sugumi, H.; Higurashi, K.; Karibe, N.; Iimura, Y.; Sasaki, A.; Kawakami, Y.; Nakamura, T.; Araki, S.; Yamanishi, Y.; Yamatsu, K. *J. Med. Chem.* **1990**, 33, 1880.
38. Villalobos, A.; Butler, T.W.; Chapin, D.S.; Chen, Y.L.; DeMattos, S.B.; Ives, J.L.; Jones, S.B.; Liston, D.R.; Nagel, A.A.; Nason, D.M.; Nielsen, J.A.; Ramirez, A.D.; Shalaby, I.A.; Frost White, W. *J. Med. Chem.* **1995**, 38, 2802.
39. Inoue, A.; Kawai, T.; Wakita, M.; Iimura, Y.; Sugimoto, H.; Kawakan, Y. *J. Med. Chem.* **1996**, 39, 4460.
40. Ishihara, Y.; Kato, K.; Goto, G. *Chem. Pharm. Bull.* **1991**, 39, 3225.
41. Fink, D.M.; Bores, G.M.; Effland, R.C.; Huger, F.P.; Kurys, B.E.; Rush, D.K.; Selk, D.E. *J. Med. Chem.* **1995**, 38, 3645.
42. Clementi, S.; Wold, S. In *Chemometric Methods in Drug Design*, van de Waterbeemd, H., Ed.; VCH, Weinheim, 1995, pp 49-62.